

RECURSIVE SELF-ORGANIZING NETWORKS FOR PROCESSING TREE STRUCTURES

Empirical Comparison

Pavol Vančo and Igor Farkaš

Department of Applied Informatics, Comenius University, Mlynská dolina, Bratislava, Slovak Republic

Keywords: Recursive self-organizing networks, Tree structures, Output representation.

Abstract: During the last decade, self-organizing neural maps have been extended to more general data structures, such as sequences or trees. To gain insight into how these models learn the tree data, we empirically compare three recursive versions of the self-organizing map – SOMSD, MSOM and RecSOM – using two data sets with the different levels of complexity: binary syntactic trees and ternary trees of linguistic propositions. We evaluate the models in terms of proposed measures focusing on unit's receptive fields and on model's capability to distinguish the trees either in terms of separate winners or distributed map output activation vectors. The models learn to topographically organize the data but differ in how they balance the effects of labels and the tree structure in representing the trees. None of the models could successfully distinguish all vertices by assigning them unique winners, and only RecSOM, being computationally the most expensive model regarding the context representation, could unambiguously distinguish all trees in terms of distributed map output activation.

1 INTRODUCTION

During the last decade, there has been an extensive research activity focused on extending self-organizing networks to more general data structures, such as sequences or trees; for overview of approaches see (Barreto et al., 2003) and (Hammer et al., 2004b). The widely used self-organizing map (SOM) (Kohonen, 1990) has been originally formulated for vectorial data (i.e. for inputs belonging to a vector space of a finite and fixed dimension). One way that allows natural processing of structured data with modified versions of SOM is to equip it with additional feedback connections. No prior metric on the structured data space is imposed, instead, the similarity measure on structures evolves through parameter modification of the feedback mechanism and recursive comparison of constituent parts of the structured data. Typical early examples of these models are the temporal Kohonen map (TKM) (Chappell and Taylor, 1993), and the recurrent SOM (RSOM) (Koskela et al., 1998). They contain units functioning as leaky integrators of their past activations, i.e. each unit has only a feedback from itself. This restriction was overcome in subsequent models, e.g. SOM for structured data (SOMSD)

(Hagenbuchner et al., 2003), merge SOM (MSOM) (Strickert and Hammer, 2005) and recursive SOM (RecSOM) (Voegtlin, 2002). These models transcend the simple local recurrence of leaky integrators and due to a more complex feedback they can represent richer dynamical behavior (Hammer et al., 2004b).

It is known that when applied to sequences, the organization of unit's receptive fields in these recursive SOM models becomes topographic and typically has Markovian nature: Sequences with similar most recent entries tend to have close representations in the map. In case of MSOM it was shown that sequences are represented by means of exponentially weighted summation of their input vectors (Hammer et al., 2004b). In RecSOM, however, also a non-Markovian dynamics was observed in case of a complex symbolic sequence such as the English text (Tiño et al., 2006). This implies a broken topography of unit's receptive fields: two sequences with the same suffix can be mapped to distinct positions on the map, separated by a region of very different suffix structure. A few years ago, extensions of these models to tree-structured data have been submitted for investigation (Hagenbuchner et al., 2003; Hammer et al., 2004b). The natural questions arise about how these models

learn to organize their receptive fields and what is their capacity in representing the trees.

In this paper, we attempt to provide answers to these questions by testing the three above mentioned SOM models (briefly introduced in Section 2) that differ by the complexity of the context representation. SOMSD uses a reference to the winner position in the grid, MSOM refers to the winner content, and RecSOM refers to the whole map activation. Unlike sequences that have linear structure, the symbolic structures naturally imply more complexity in data organization and, as we will explain later, one can differentiate between the content and the structure in a tree. For the purpose of empirical comparison, we propose two pairs of related quantitative measures (Section 3). We assess and compare the performance of the three models on two data sets that differ in complexity: binary syntactic trees and ternary trees of linguistic propositions (Section 4).

2 MODELS

As proposed in (Hammer et al., 2004a), all three models can be generalized to processing n -ary trees ($n = 1$ applies to sequences). In each model, a unit $i \in \{1, 2, \dots, N\}$ in the map has $n + 1$ weight vectors associated with it: $\mathbf{w}_i \in \mathcal{R}^M$ – weight vector linked with an M -dimensional input $\mathbf{s}(t)$ feeding the network at time t , and $\mathbf{c}_i^{(j)}$ – j th context weight vector ($j = 1, 2, \dots, n$) linked with the context whose dimensionality is model-dependent.

For each model, the distance of unit i from a tree at time t is computed as

$$d_i(t) = \alpha \|\mathbf{s}(t) - \mathbf{w}_i\|^2 + \beta \sum_{j=1}^n \|\mathbf{p}_{ch(j)} - \mathbf{c}_i^{(j)}\|^2 \quad (1)$$

where parameters $\alpha > 0$ and $\beta > 0$ respectively influence the effect of the current input and the context on the neuron's profile, $\|\cdot\|$ denotes the Euclidean distance, $ch(j)$ denotes the winner index for j th child, $\mathbf{c}_i^{(j)}$ is i th context (weight) vector of j th child, and $\mathbf{p}_{ch(j)}$ is the (model-specific) context representation. For SOMSD, $\mathbf{p}_{ch(j)} \equiv \mathbf{r}_{ch(j)}$ is a two-dimensional vector (we assume 2D maps) with integer components specifying the winner location in the grid. For MSOM, $\mathbf{p}_{ch(j)} \equiv \mathbf{q}_{ch(j)}$, where the so called context descriptor of j th child is computed as

$$\mathbf{q}_{ch(j)} = (1 - \gamma) \mathbf{w}_{ch(j)} + \gamma \frac{1}{n} \sum_{j'=1}^n \mathbf{c}_{ch(j)}^{(j')}$$

Hence, the dimensionality of $\mathbf{q}_{ch(j)}$ equals input dimension M . Finally, for RecSOM, $\mathbf{p}_{ch(j)} \equiv \mathbf{y} =$

$[y_1, y_2, \dots, y_N]$ is the output activation of RecSOM with components

$$y_i(t) = \exp(-d_i(t)). \quad (2)$$

The dimensionality N of the $\mathbf{p}_{ch(j)}$ (for each child) makes RecSOM computationally the most expensive architecture. The activation function in Eq. 2 is also used for the other two models to provide map output activation vectors that we need for model comparison.

Learning of both input and context weights in each model has the same Hebbian form as in the standard SOM (Hammer et al., 2004a):

$$\begin{aligned} \Delta \mathbf{w}_i &= \mu h(i, i^*) (\mathbf{s}(t) - \mathbf{w}_i), \\ \Delta \mathbf{c}_i^{(j)} &= \mu h(i, i^*) (\mathbf{p}_{ch(j)}(t) - \mathbf{c}_i^{(j)}) \end{aligned}$$

where $j = 1, 2, \dots, n$, the winner $i^* = \arg \min_i \{d_i(t)\}$, μ is the learning rate, $h(i, i^*) = \exp(-d(i, i^*)/\sigma^2)$ is the neighborhood function that uses $d(\cdot, \cdot)$ as the Euclidean distance of the two units in the lattice. The “neighborhood width”, σ , linearly decreases to allow forming topographic representation of the trees.

3 PERFORMANCE MEASURES

In order to evaluate the model performance we introduced two pairs of related numerical measures. The first measure was inspired by the quantizer depth introduced for symbolic sequences for quantifying the amount of memory captured by the map (Voegtlin, 2002). It is defined as the average size of the unit's receptive field, i.e. the common suffix of all sequences for which that neuron becomes the winner. In case of trees, we propose an analogue named Tree Quantizer Depth (TQD), computed as the average size of Tree Receptive Field (TRF), i.e. the common “suffix” (subtree) of all vertices for which that neuron is the winner. Hence,

$$\text{TQD} = \sum_{i=1}^N p_i s_i \quad (3)$$

where p_i is the probability of unit i becoming a winner (in a given data set) and s_i is the (integer) size of its TRF. TQD is sensitive to the content (of tree leaves) and returns the value of an average tree depth captured by the individual map units (functioning as subtree detectors).

Unlike sequences, which have linear structure, trees provide room for distinguishing between the content (captured by TQD) and the structure only. This leads to the second measure, the Structure-only sensitive TQD (STQD), which detects the structure of a tree by only distinguishing between the leaves and

the inner nodes, not between the nodes with different labels (i.e. their content). (For example, a unit can become sensitive to a tree $a(b -)$), i.e. it is insensitive to the contents of the right child, being an inner tree node). STQD is defined as

$$\text{STQD} = \sum_{i=1}^N p_i s'_i \quad (4)$$

where s'_i denotes STRF of i th neuron and p_i is the same as above.

The other pair of measures was introduced to quantify the discrimination capacity of the models to unambiguously represent different trees. This implies the ability to uniquely represent all vertices (subtrees) contained in all trees (Hammer et al., 2004b). One view of the vertex representation is in terms of a separate winner reserved for it. The alternative view is based on a distributed representation of vertices that entails the overall map output activation. The proposed measures focus on these alternatives.

So, the third measure – the winner differentiation (WD) refers to the level of winners and is computed as the ratio of the number of different winners identified and the number of all different subtrees in the data set (including the leaves), that is

$$\text{WD} = \frac{|\{j | \exists t : j = i^*(t)\}|}{|\{\text{vertices_in_data_set}\}|} \quad (5)$$

$\text{WD} < 1$ indicates that not all vertices could be distinguished by the map (i.e. two or more different vertices would share the winner). The fourth, more “detailed” measure looks at the differences between map output activation vectors, and yields the difference between the two most similar representations (probably corresponding to two very similar trees such as $v(d(an))$ and $v(dn)$). We will refer to this measure as the normalized minimum Euclidean distance

$$\text{MED} = \arg \min_{u \neq v} \{\|\mathbf{y}(T_u) - \mathbf{y}(T_v)\|/N\}, \quad (6)$$

where $\mathbf{y}(T_z)$ is the map output activation vector (whose components are obtained using Eq. 2) corresponding to processing of the root of the tree T_z . $\text{MED} > 0$ implies that all vertices can be distinguished in terms of map output activation vectors.

4 EXPERIMENTS

We tuned the model parameters experimentally according to the task difficulty. We started with basic maps of 10×10 units in case of binary trees and 15×15 units for ternary propositions. We looked for the models with the best discrimination capacity as

determined by the largest number of unique winners in representing different vertices (captured by WD measure). We also tested larger maps with 225 and 400 units using the optimal parameters (α, β) found for the initial map size. In MSOM, the parameter of the context descriptor was set to its default value $\gamma = 0.5$ in both experiments. In all simulations, the leaves were assigned localist (one-hot) codes (to be treated as symbols). We systematically searched the (α, β) parameter space, as each model can trade-off the effect of leaves and contexts. It was observed that increasing α (while keeping β constant) did not affect output representations of leaves but led to the overall decrease of activations for trees. Increasing β (with constant α) led to gradual vanishing of output representations of leaves, and to focusing of activations for trees (and also vanishing in combination with higher α).

4.1 Binary Syntactic Trees

This data set contained 7 syntactic trees with labeled leaves and unlabeled inner nodes (vertices) (Table 1). The trees were generated by a simple grammar originally developed for testing the representational capacity of the Recursive Auto-Associative Memory (Pollack, 1990). For the RAAM, being a two-layer perceptron trained as auto-associator, the ability to represent a tree involves its successful encoding (at the hidden layer) and the subsequent unambiguous decoding (at the output layer). In case of our unsupervised feedback maps, there is only the encoding part. The ability of the map to represent a tree implies its ability to also uniquely represent all vertices (subtrees) contained in the training set (listed in the right half of Table 1).

Similarly to RAAM, processing a tree in a feedback map proceeds bottom-up from the leaves, for which context activations are set to zero vectors, up to the root. When processing the inner nodes, the inputs $\mathbf{s}(t)$ are set to zero vectors. Intermediate results (activations $\mathbf{p}_{ch(j)}$) are stored in a buffer to be retrieved later. The weights are updated in each discrete step.

The models were trained for 2000 epochs. During the first 60% of epochs, the neighborhood width was set to linearly decrease, $\sigma: 3 \rightarrow 0.5$ (ordering phase), and was then kept constant (fine-tuning phase). For the larger maps the initial neighborhood width was proportionally increased and the profile was kept the same. The learning rate linearly decreased $\mu: 0.3 \rightarrow 0.1$ during the ordering phase, and was then kept constant. For the best models of all sizes, we present the four quantitative measures (averaged over 100 runs) in Tables 2 and 3 and also the (typical) graphical information about unit weights and output activations. Stan-

Table 1: Binary trees used for training and the list of vertices comprised by the data set.

Training set		Vertices contained in it	
$(d(a(a(an))))$	$((dn)v)$	(an)	$(p(dn))$
$((dn)(p(dn)))$	$((dn)(v(d(an))))$	$(a(an))$	$(d(an))$
$(v(dn))$	$((d(an))(v(p(dn))))$	$(a(a(an)))$	$(v(d(an)))$
$(p(d(an)))$		(dn)	$(v(p(dn)))$

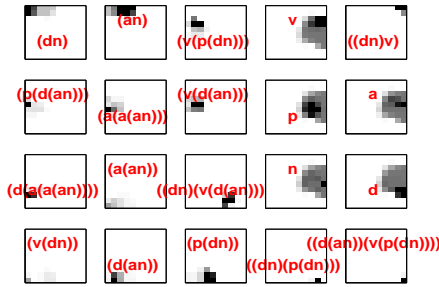


Figure 1: Output activities of SOMSD for all vertices from the binary trees data set ($\alpha = 0.5, \beta = 0.9$).

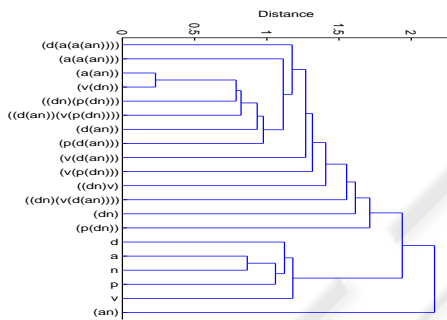


Figure 2: Dendrogram of SOMSD output activations for all vertices from the binary trees data set.

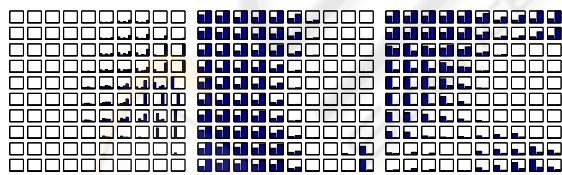


Figure 3: Converged (a) input, (b) left context and (c) right context weights of the SOMSD model trained on the binary trees. Topographic organization is evident in all cases.

dard errors were negligible in all cases except MED in SOMSD. All these characteristics illustrate model's behavior and together facilitate model comparison.

SOMSD. The best results for SOMSD were obtained using $\alpha = 0.5$ and $\beta = 0.9$. The average percentage of (possible) unique winners was almost 93% (Table 3). The errors were caused by similar trees (such as $(a(an))$ and $(v(dn))$) that shared the win-

ners. The SOMSD output activity (Figure 1) and the unit's weight profiles (Figure 3) clearly show the topographic organization in which the winners for leaf nodes are clearly separated from winners for trees. In addition, simpler trees, located in the upper left area, are separated from the more complex trees in the bottom right area of the map. It can also be observed that activation profiles for trees are more focused than profiles for leaves. The corresponding dendrogram of the map activity (Figure 2) reveals how the map differentiates between the trees. Leaves are differentiated from non-trivial trees with an exception of (an) which is the simplest tree. Increasing the map size was observed to lead to an improvement (Table 3): all 20 trees could be, with a rather high reliability, distinguished in the map. Only SOMSD displayed non-zero variability of all measures.

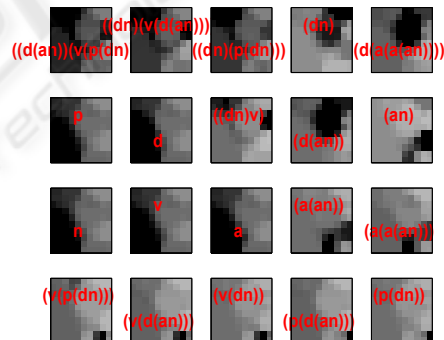


Figure 4: Output activities of MSOM for all vertices from the binary trees data set ($\alpha = 0.2, \beta = 1.0$).

MSOM. As seen in Figure 4, winners for leaves (trivial trees) are again well separated from units representing trees. There are only 80% of different winners, because each neuron becomes activated for several inputs – the MSOM activation is much more widespread than in the case of SOMSD (and RecSOM).

Even though the dendrogram (Figure 5) shows that MSOM differentiates between leaves and non-trivial trees, the trees are differentiated differently from SOMSD model. The weight profiles (Figure 6) split the map in representing leaves and inner nodes. The differences between the left and the right contexts are due to the asymmetry of the trees in the data set

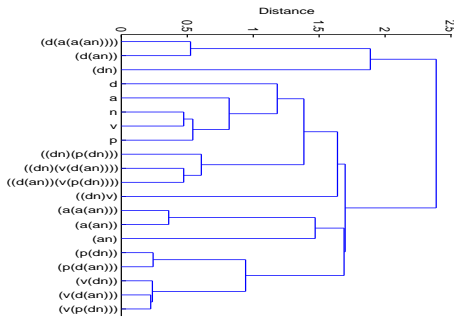


Figure 5: Dendrogram of MSOM output activations for all vertices from the binary trees data set.

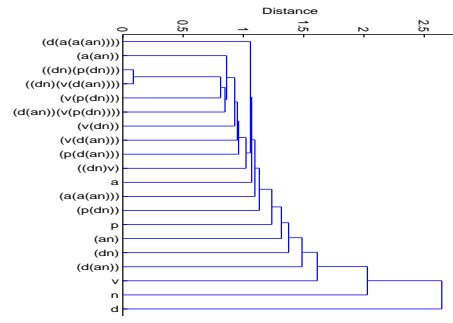


Figure 8: Dendrogram of RecSOM output activations for all vertices from the binary trees data set.

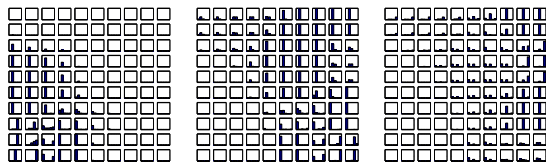


Figure 6: Converged (a) input, (b) left context and (c) right context weights of the MSOM model trained on the binary trees.

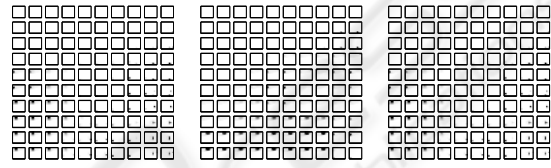


Figure 9: Converged (a) input, (b) left context and (c) right context weights of the RecSOM model trained on the binary trees. The context weights are displayed as 2D mesh plots.

(left and right children). Increasing the map size to 225 units led to an improvement of all measures (except MED). Further increase to 400 units (i.e. almost the double size) did not improve any measure value. The problem for all MSOMs was to differentiate between $(v(d(an)))$ and $(v(dn))$ even in this simple data set.

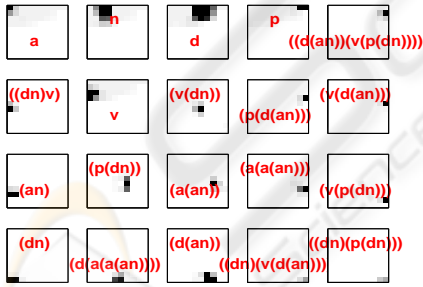


Figure 7: Output activities of RecSOM for all vertices from the binary trees ($\alpha = 1.6, \beta = 0.9$).

RecSOM. Best results were achieved with $\alpha = 1.6$ and $\beta = 0.9$. This parameter combination differs from the other two models due to the opposite $\alpha:\beta$ ratio. The likely reason is that higher value of α in RecSOM is needed to counterbalance the effect of high-dimensional context activations. Nevertheless, the output activations of leaf nodes remained very weak even after training. The whole map activity (Figure 7) is more focused than in the case of MSOM and SOMSD but there are more different winners, 95%

on average for the initial map size. The dendrogram of RecSOM (Figure 8) is different from the previous models because the differentiation is not hierarchical and some leaves are mingled with trees. The reason lies in highly focused output activations. The weight profiles (Figure 9) show that units focusing on leaves are again well separated from units focusing on trees. As with SOMSD, increasing the map size to 225 units led to maximum WD = 1.0 (100%) and to an increase of MED as well.

In all models, the values of TQD and STQD measures are quite similar suggesting that for this data set the models do not differ in the average depth of their unit's receptive fields. These values are close to 3, i.e. an average unit is sensitive to a vertex with two children. In addition, STQD is similar to TQD which implies that maps did not develop detectors sensitive for tree structures only. The likely reason is a low number of leaves and a small size of the data set.

Table 2: TQD and STQD (in parantheses) measures for the models trained on the binary trees.

Model	10×10	15×15	20×20
SOMSD	2.82 (2.92)	2.93 (2.93)	2.93 (2.93)
MSOM	2.61 (2.66)	2.86 (2.86)	2.86 (2.86)
RecSOM	2.83 (2.86)	2.93 (2.93)	2.93 (2.93)

Table 3: WD and MED (in parantheses) measures for the models trained on the binary trees.

Model	10×10	15×15	20×20
SOMSD	0.93 (0.003±0.002)	1.00 (0.0005)	0.99 (0.002±0.001)
MSOM	0.80 (0.002)	0.95 (0.002)	0.95 (0.001)
RecSOM	0.95 (0.0008)	1.00 (0.004)	1.00 (0.002)

4.2 Ternary Linguistic Propositions

This data set originated from English sentences that were generated using a probabilistic context-free grammar with semantic constraints and were then rewritten into ternary propositions. The translation process resulted in 307 various (non-trivial) trees with maximum depth 7. Table 4 lists a few examples of used sentences and their translations to propositions.¹ Some trees have empty inner nodes (NULL labels). The fifty words (i.e. leaves) in the lexicon yield $M = 50$. We trained the maps with 15×15 units for 20 epochs. The neighborhood size was set to $\sigma:5 \rightarrow 0.5$ over 12 epochs and then remained constant. For larger maps, σ was proportionally increased. The learning rate was set to $\mu:0.3 \rightarrow 0.1$ over 12 epochs, and was then kept constant.

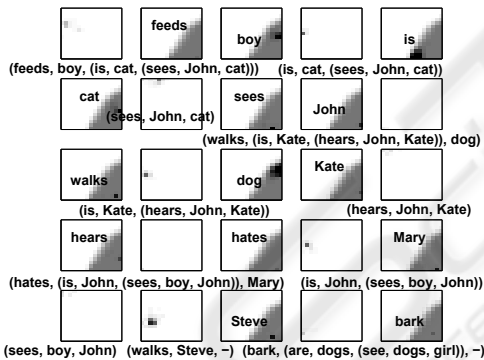


Figure 10: Output activities of SOMSD for 25 randomly selected vertices from the ternary trees data set. Longer tree labels are positioned below the corresponding image.

SOMSD. For the best map ($\alpha = 0.5, \beta = 0.4$), almost 20% of all inputs had a unique winner. The SOMSD behavior clearly differentiates between leaves and non-trivial trees (Figure 10). The winners for leaves, located in the lower right corner, show little differences in their map output representations. In the case of leaves the activity of the map is less focused than for more complex trees. The more complex a tree, the more focused activity is devoted to it in the map. A

¹In translation, the word who was replaced by the heads is and are depending on the subject number used in the phrase. For a sentence with maximum embedding of depth n , the tree depth is $2n + 1$.

more detailed analysis revealed that SOMSD learned to differentiate non-trivial trees based on depth², as predicted in (Hammer et al., 2004b). The number of winners in SOMSD oscillated between 71 and 66. Despite fewer winners, the runs with 66 winners (30% of cases) yielded better results in terms of TQD and STQD. Increasing the map size to 20×20 led to an increase of all measures except MED that remained 0. This means that SOMSD cannot distinguish some inputs even at the level of the map activation.

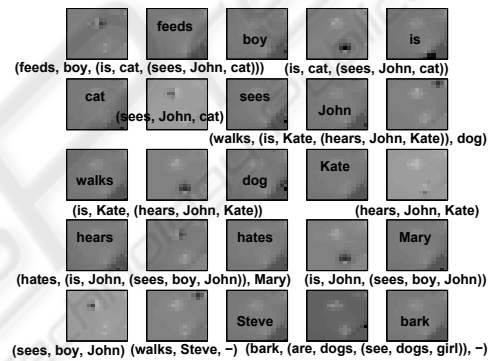


Figure 11: Output activities of MSOM for 25 randomly selected vertices from the ternary trees data set. Longer tree labels are positioned below the corresponding image.

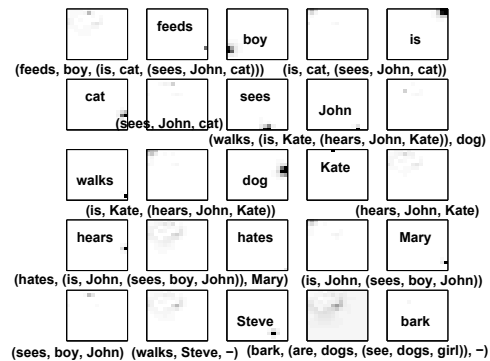


Figure 12: Output activities of RecSOM for 25 randomly selected vertices from the ternary trees data set. Longer tree labels are positioned below the corresponding image.

²Illustrating dendrograms for this data set are not included here due to space limitations.

Table 4: Examples of simpler generated sentences and their translations.

Sentence	Proposition
Steve walks	(walks Steve NULL)
women see boys	(see women boys)
dogs who_pl see girl bark	(bark (are dogs (see dogs girl)) NULL)
boy feeds cat who John sees	(feeds boy (is cat (sees John cat)))

MSOM. The best results were achieved for $\alpha = 0.4$ and $\beta = 0.6$. Parameter β needed to be slightly larger than in SOMSD, because the context weights have higher dimension. It can be seen that MSOM activity (Figure 11) is quite different from that of SOMSD. The whole map is activated for every input although most of the neurons show only low activity. Leaves are located in the lower right part of the map and non-trivial trees are scattered throughout the rest of the map. The analysis of output activation dendrograms revealed that MSOM differentiates trees with respect to both labels and the depth. Regarding the labels, the first (topmost) word (being a verb) became the clustering parameter. The best result for MSOM was 53 distinct winners (8.3%) which is far below SOMSD. Both memory depth measures were even further decreased after enlarging the map size to 20×20 units. Based on these measures, the performance of the MSOM model was the worst among all models for the ternary trees data set.

RecSOM. The best results for RecSOM were achieved for $\alpha = 2.4$ and $\beta = 0.4$. The map activations (Figure 12) are more focused for both leaves and trees to the previous models, and also the organization of output space is very different. Leaves are not located in one part of the map but are scattered across the map. The leaves usually have different representations than the rest of inputs. As in previous models, both the most recent inputs and the structure are important for the map activation. Regarding the output activations, both the structure and RFs influence the output representations.

In sum, regarding the memory depth, the models already show differences in terms of TQP, where RecSOM ranks first. In addition, values for STQD are significantly higher in all models which implies that units also developed sensitivity to structures. The reason may be in both higher number of possible trees and the number of leaves such that units can no longer cope with the content sensitivity given the available resources (number of units). Regarding the uniqueness of representations, with respect to winners, SOMSD was the best model for this data set. However, RecSOM was the only model that achieved $MED > 0$, i.e. was able to distinguish every single vertex in terms of map output activation. We can con-

Table 5: Average TQD and STQD (in parantheses) measures for all models trained on the ternary trees data set.

Model	15×15	20×20
SOMSD	1.10 (2.65)	1.14 (2.90)
MSOM	0.76 (1.63)	0.54 (1.67)
RecSOM	1.17 (1.69)	1.40 (2.26)

Table 6: Average WD and MED (in parantheses) measures for all models trained on the ternary trees data set.

Model	15×15	20×20
SOMSD	0.195 (0.0)	0.241 (0.0)
MSOM	0.083 (0.0)	0.050 (0.0)
RecSOM	0.160 (1.4×10^{-6})	0.171 (2.4×10^{-6})

clude that RecSOM benefits from the higher complexity of its context representation.

It is true that SOMSD is computationally the most efficient architecture and was even advocated as the most appropriate model (Hammer et al., 2004b) judging from comparisons in representing company logos (presented as tree structures). Our simulations favour RecSOM, instead, since the high complexity of its context representation seems justified in case of ternary propositions. Of course, further simulations are required to verify these claims.

5 CONCLUSIONS

The goal of this paper was to shed light onto how different recursive SOM models process tree structured data. We compared the performance of these models using four proposed quantitative measures. With respect to content memory depth (TQD), it is not possible to say which model performs best regarding both data sets because the performance of RecSOM and SOMSD is comparable. Regarding the structure (STQD), SOMSD yields the best results suggesting that it can cluster the trees very well according to their structural properties. The models differ in the way how they distinguish the trees. For SOMSD, the tree structure is more important than the content (of the labels), but the content also plays a role within the same structure. MSOM clusters the trees in the map more preferably by the content than SOMSD but the

structure is also important. RecSOM model creates a complex organization of tree representations based on both the structure and the content.

Regarding the uniqueness of output representations, it turns out that the winner position is only sufficient in the case of simple tree data sets such as the binary syntactic trees. Although according to the theoretical claim (Hammer et al., 2004b) we should only need a sufficient number of neurons to unambiguously represent all vertices, our experimental simulations suggest that the sufficient map size is the necessary but not the sufficient condition. The problem appears to lie in finding weights (by training) that would lead to unique winners. Therefore, we have to employ the map output activation for tree representation, as suggested by simulations. However, this only helps in case of RecSOM that yields nonzero differences in all pairs of map output activations for both data sets. Hence, RecSOM benefits from higher complexity of its context representation.

Understanding how recursive SOMs (and neural networks in general) learn to represent the data structures is not only important for practical tasks, but also in cognitive science as a principled paradigm based on neural computation. Connectionist models have been criticised for lacking important representational properties (that can be found in symbolic models) such as those needed for systematic representation and processing of structures (Fodor and Pylyshyn, 1988). Nevertheless, neural networks do offer the potential to process symbolic structures employing various types of recursive architectures (Hammer, 2003). However, further investigations are needed.

ACKNOWLEDGEMENTS

This work was supported by Slovak Grant Agency for Science. I.F. is also part-time with Institute of Measurement Science, Slovak Academy of Sciences.

REFERENCES

- Chappell, G. J. and Taylor, J. G. (1993). The temporal Kohonen map. *Neural Networks*, 6:441–445.
- de A. Barreto, G., Araújo, A., and Kremer, S. (2003). A taxonomy of spatiotemporal connectionist networks revisited: The unsupervised case. *Neural Computation*, 15:1255–1320.
- Hagenbuchner, M., Sperduti, A., and Tsoi, A. (2003). A self-organizing map for adaptive processing of structured data. *IEEE Transactions on Neural Networks*, 14(3):491–505.
- Hammer, B., Micheli, A., Sperduti, A., and Strickert, M. (2004a). Recursive self-organizing network models. *Neural Networks*, 17(8-9):1061–1085.
- Hammer, B., Micheli, A., Strickert, M., and Sperduti, A. (2004b). A general framework for unsupervised processing of structured data. *Neurocomputing*, 57:3–35.
- Kohonen, T. (1990). The self-organizing map. *Proceedings of the IEEE*, 78(9):1464–1480.
- Koskela, T., Varsta, M., Heikkonen, J., and Kaski, K. (1998). Time series prediction using recurrent SOM with local linear models. *International Journal of Knowledge-Based Intelligent Eng. Systems*, 2(1):60–68.
- Strickert, M. and Hammer, B. (2005). Merge SOM for temporal data. *Neurocomputing*, 64:39–72.
- Tiño, P., Farkaš, I., and van Mourik, J. (2006). Dynamics and topographic organization in recursive self-organizing map. *Neural Computation*, 18:2529–2567.
- Voegtlin, T. (2002). Recursive self-organizing maps. *Neural Networks*, 15(8-9):979–992.
- Pollack, J. (1990). Recursive distributed representations. *Artificial Intelligence*, 46(1-2):77–105.
- Fodor, J.A., and Pylyshyn, Z.W. (1988). Connectionism and cognitive architecture: A critical analysis. *Cognition*, 28: 3–71.
- Hammer, B. (2003). Perspectives on learning symbolic data with connectionistic systems. In: *Adaptivity and Learning*, Springer, 141–160.